Journal of Molecular Medicine (2018) 96:1407–1418
https://doi.org/10.1007/s00109-018-1704-z

JMolMed

ORIGINAL ARTICLE

Pre-treatment with angiotensin-(1–7) inhibits tumor growth via autophagy by downregulating PI3K/Akt/mTOR signaling in human nasopharyngeal carcinoma xenografts

Yu-Tsai Lin[1,2,3] · Hung-Chen Wang[4] · Hui-Ching Chuang[1,2] · Yi-Chiang Hsu[5] · Ming-Yu Yang[1,6] · Chih-Yen Chien[1,2]

Received: 26 June 2018 / Revised: 1 October 2018 / Accepted: 10 October 2018 / Published online: 29 October 2018

Abstract

The highest incidence of nasopharyngeal carcinoma (NPC) is in southeast China, including Taiwan. Many side effects have been observed following radiation therapy with chemotherapy; hence, exploring new treatment modalities for NPC is an important future direction. Angiotensin-(1–7) [Ang-(1–7)] is an endogenous heptapeptide hormone and important component of the renin–angiotensin system that acts through both the Mas receptor and AT2 receptor, exhibiting anti-proliferative and anti-angiogenic properties in cancer cells. However, the anti-cancer activity of Ang-(1–7) related to autophagy in NPC remains largely debated. The effects and signaling pathway(s) involved in the Ang-(1–7)/Mas receptor axis in NPC were investigated both in vitro and in vivo. Ang-(1–7) inhibited cell proliferation, migration, and invasion in NPC-TW01 cells. Ang-(1–7) induced autophagy by increasing the levels of the autophagy marker LC3-II and by enhancing p62 degradation via activation of the Beclin-1/Bcl-2 signaling pathway with involvement of the PI3K/Akt/mTOR and p38 pathways in vitro study. In addition, pre-treatment with Ang-(1–7) inhibited tumor growth in NPC xenografts by inducing autophagy, suggesting a correlation between PI3K/Akt/mTOR pathway inhibition and the abovementioned anti-cancer activities. However, no autophagy was observed following Ang-(1–7) post-treatment. Taken together, these data indicate that Ang-(1–7) plays a novel role in autophagy downstream signaling pathways in NPC, supporting its potential as a therapeutic agent for alleviation the incidence of NPC and preventive treatment of recurrent NPC.

Ming-Yu Yang and Chih-Yen Chien contributed equally to this work.

Electronic supplementary material The online version of this article (https://doi.org/10.1007/s00109-018-1704-z) contains supplementary material, which is available to authorized users.

✉ Ming-Yu Yang
yangmy@mail.cgu.edu.tw

✉ Chih-Yen Chien
cychien3965@adm.cgmh.org.tw

Yu-Tsai Lin
xeye@cgmh.org.tw

Hung-Chen Wang
m82whc@gmail.com

Hui-Ching Chuang
entjulia@cgmh.org.tw

Yi-Chiang Hsu
jenway@mail.cjcu.edu.tw

[1] Department of Otolaryngology, Kaohsiung Chang Gung Memorial Hospital and Chang Gung University College of Medicine, 123 Ta-Pei Road, Niao-Song District, Kaohsiung 833, Taiwan

[2] Kaohsiung Chang Gung Head and Neck Oncology Group, Cancer Center, Kaohsiung Chang Gung Memorial Hospital, Kaohsiung, Taiwan

[3] College of Pharmacy and Health Care, Tajen University, Pingtung County, Taiwan

[4] Department of Neurosurgery, Kaohsiung Chang Gung Memorial Hospital, Kaohsiung, Taiwan

[5] Department of Medical Sciences Industry and Innovative Research Center of Medicine, College of Health Sciences, Chang Jung Christian University, Tainan, Taiwan

[6] Graduate Institute of Clinical Medical Sciences, College of Medicine, Chang Gung University, Taoyuan City, Taiwan

Key messages

- Ang-(1–7) inhibits cell proliferation, migration, and invasion by activating autophagy
- Ang-(1–7)pre-treatment inhibits tumor growth via autophagy by suppressing PI3K/Akt/mTOR pathway.
- Ang-(1–7) may provide a novel preventative treatment for NPC and recurrent NPC

Keywords Nasopharyngeal carcinoma · Angiotensin-(1–7) · Autophagy · PI3K/Akt/mTOR signaling · Pre-treatment

Introduction

The standard incidence of nasopharyngeal carcinoma (NPC) worldwide is 1.2 per 100,000 (1.7 per 100,000 men and 0.7 per 100,000 women) and is especially high among the Chinese population [1]. The peak age of NPC incidence is 50–60 years [2]. The most important risk factors for NPC are genetic predisposition, Epstein–Barr viral infection, and dietary and environmental factors [3]. NPC is a prevalent disease in Taiwan [4]. Radiotherapy or radiotherapy combined with chemotherapy is the mainstay of treatment [4]; however, severe side effects, such as sensorineural hearing loss, mucositis, dry mouth, and dietary problems, as well as the limitations of conventional treatments have led to the widespread application of complementary and/or alternative medicines. Furthermore, the local recurrence rate of NPC after initial radiotherapy is approximately 10%. Re-irradiating the same field may cause potentially serious side effects and complications. The treatment of recurrent NPC remains a challenging clinical problem [5, 6]. Therefore, it is necessary to identify new therapeutic methods for NPC and recurrent NPC.

The renin–angiotensin system (RAS) is an endocrine system that plays a central role in cardiovascular and renal physiology by regulating blood pressure and sodium balance [7]. One member of the "alternative RAS axis" is the angiotensin-(1–7) [Ang-(1–7)] peptide, which is generated by subsequent cleavage of angiotensin II by angiotensin-converting enzyme 2. Ang-(1–7) binds to G protein-coupled receptors, namely, the Mas receptor (MasR), which activates distinct signaling pathways that lead to cellular effects [8]. In cancer, Ang-(1–7) is an anti-proliferative and anti-angiogenic molecule that mediates its effects by binding to MasR [9, 10]. In vitro studies on lung cancer cells have confirmed the anti-proliferative function of Ang-(1–7) via MasR. Ang-(1–7) inhibits cell migration and invasion by inactivating the PI3K/Akt, p38 and JNK signaling pathways [11, 12]. In vivo studies have indicated that administration of Ang-(1–7) reduces lung and prostate tumor xenografts [13, 14], as well as prostate cancer metastasis [15]. Furthermore, a recent report showed that Ang-(1–7) downregulated the AT1 receptor (AT1R) mRNA level, upregulated AT2 receptor and MasR mRNA levels and p38-MAPK phosphorylation, and suppressed communication between H22 hepatocellular carcinoma and endothelial cells, which may provide a novel and promising approach for the treatment of hepatocellular carcinoma [16]. As noted above, Ang-(1–7) may promote tumor cell death by regulating the stoichiometry of the receptors and subsequently altering their signaling. Moreover, autophagy (type II programmed cell death) is a major intracellular pathway via the degradation and recycling of proteins, ribosomes and organelles [17]. Autophagy as a novel cancer therapy is an effective approach used to alleviate treatment resistance in apoptosis-defective tumor cells [18]. Ang-(1–7) acts as a tumor suppressor, making it a promising therapeutic target.

In a study on Ang-(1–7) in NPC, Pei et al. indicated that Ang-(1–7) inhibits the proliferation of human NPC cells and reduces human nasopharyngeal xenograft growth and tumor angiogenesis [19]. These results suggest that Ang-(1–7) could serve as a novel anti-angiogenic treatment and potential target gene for NPC therapy. However, the effects of Ang-(1–7) on autophagic activity in NPC remain unclear. In the present study, we investigated the regulatory mechanisms of Ang-(1–7) on NPC cells in vitro and two NPC tumor xenograft models (pre- and post-treatment) in vivo. Our data suggest that Ang-(1–7) is a potential novel therapeutic agent for NPC because it exerts autophagic activity.

Materials and methods

Materials

Dulbecco's modified Eagle's medium (DMEM), fetal bovine serum (FBS), phosphate-buffered saline (PBS), sodium pyruvate, trypsin, and antibiotics were purchased from Gibco, BRL (Grand Island, NY, USA). 3-(4,5-Dimethylthiazol-2-yl)-2,5-diphenyltetrazolium bromide (MTT), dimethyl sulfoxide (DMSO), and the MasR antagonist A779 were purchased from Sigma-Aldrich (St. Louis, MO, USA). Matrigel (Basement Membrane Matrix) was purchased from BD Biosciences (Franklin Lakes, NJ, USA). The specific inhibitor 3-methyladenine (3-MA) was purchased from Merck Millipore (Merck KGaA, Darmstadt, Germany). All reagents and compounds were of analytical grade.

Cell culture

The human NPC cell line NPC-TW 01 was provided by Prof. Chin-Tarng Lin (National Taiwan University, Taipei, Taiwan). Cells were cultured in growth medium (DMEM supplemented

with 10% FBS, 100 kU/L penicillin and 100 mg/L streptomycin) at 37 °C and 5% CO_2 in a humidified atmosphere.

Cell proliferation assay

Cells were seeded in a 96-well culture plate at 5000 cells/well. MTT (1 mg/ml) was added to each well for at least 4 h. The reaction was stopped by the addition of DMSO, and optical density was measured at 570 nm on a multi-well plate reader.

Wound healing assay

The cell density was adjusted to 2.5×10^5/ml. Cells were seeded in 35-mm culture dishes with silicon inserts consisting of two chambers separated by a 500-μm wall (ibidi GmbH, Munich, Germany). After overnight incubation at 5% CO_2 at 37 °C for 24 h, the silicon inserts were removed. Cells were treated with Ang-(1–7) and A779 and incubated for 0, 24, 48 or 72 h. Wound healing was observed by 200× phase-contrast microscopy (Olympus CKX41, Tokyo, Japan) in three independent experiments. Images evaluated using Image-Pro Plus 6.0 software (Media Cybernetics, Rockville, MD, USA) were used to calculate the mean ± standard deviation. Cell migration is expressed as wound closure, and each group was compared with the control group (0 h).

Transwell invasion assay

The cell density was adjusted to 2.5×10^5/ml. Cells were seeded in the upper chamber of a 24-well Transwell chamber (Corning Life Sciences, Corning, NY, USA) with 50 μl Matrigel™ (BD Biosciences). Complete medium (750 μl) was added to the lower chamber. The plate was incubated at 37 °C for 18–24 h. Cells were fixed with 3.7% paraformaldehyde for 2 min and permeabilized with 100% methanol for 20 min at room temperature. Cells were then stained with 0.1% crystal violet solution for 20 min and washed twice with PBS. Non-invasive cells were removed with a cotton swab. Cell numbers were counted using phase-contrast microscopy, and the mean value was used as the number of invasive cells. The experiment was repeated three times. Images measured using Image-Pro Plus 6.0 software were used to calculate the mean ± standard deviation. Invasion suppression rate = [(penetration cell number in the control group − penetration cell number in the treated group)/penetration cell number in the control group] × 100%.

Small-interfering RNA (siRNA) transfection

Plasmids expressing siRNA specifically targeting Bcl-2 or control siRNA (no silencing) were designed and synthesized (Stealth RNAi, Invitrogen, Thermo Fisher Scientific, Waltham, MA, USA) to knockdown the expression of Bcl-2. Confluent cells were cultured in serum-free DMEM for 24 h before transfection, which was conducted in 24-well plates using 50 nM siRNAs and Lipofectamine 2000 (Invitrogen, Carlsbad, CA, USA) according to the manufacturer's protocol. After 48–72 h of siRNA incubation, cells were harvested for further analyses. Bcl-2 knockdown was confirmed by Western blotting.

In vivo tumor xenograft mouse models

Male nude mice (5–7 weeks old) were maintained according to the Institutional Animal Care and Use Committee (IACUC) of the Animal Experimentation in Kaohsiung Chang Gung Memorial Hospital, Kaohsiung, Taiwan. Two treatment models were established. In the first model (post-treatment group), NPC-TW-01 cells (1×10^7 in 0.1 ml PBS) were injected into the right upper back of each mouse. When the tumors grew to 50 mm^3 in size, the mice were randomly divided into four treatment groups: mock group (equal volume saline), low-dose Ang-(1–7) (0.2 μg/kg), high-dose Ang-(1–7) (1 μg/kg), or Ang-(1–7) (1 μg/kg) + A779 (1 μg/kg). All drugs were subcutaneously injected once each day. In the second model (pre-treatment group), mice were randomly divided into five groups: mock group, low-dose Ang-(1–7) (0.2 μg/kg), high-dose Ang-(1–7) (1 μg/kg), Ang-(1–7) (1 μg/kg) + A779 (1 μg/kg), or Ang-(1–7) (1 μg/kg) + 3-MA (5 μg/kg). Cells were pre-treated for 2 weeks, and NPC-TW-01 cells were subcutaneously inoculated into the back of each mouse. Drug treatment was continued once a day for 4 weeks. After 6 weeks, all mice were euthanized, and the tumors were collected for subsequent experiments. The methods used in the animal experiments were performed in accordance with relevant guidelines. All animal studies were approved by the IACUC of Kaohsiung Chang Gung Memorial Hospital, Kaohsiung, Taiwan (IACUC approval number 2016121913).

Immunohistochemistry and immunofluorescence staining

Tumor sections (4 μm) were prepared on slide glasses, and sectioned slides were deparaffinized in xylene and gradually hydrated using an alcohol gradient from 100 to 70%. After washing with PBS, slides were warmed in a microwave with citrate buffer following incubation in 3% H_2O_2. Sections were then incubated with 5% bovine serum albumin in PBS to block nonspecific binding. Ki67 (1:100, ab15580; Abcam, Cambridge, UK) and microtubule-associated protein 1A/1B-light chain 3 (LC3-II) (1:200, L7543; Sigma-Aldrich) antibodies were added to the slides and incubated overnight at 4 °C. Sections were then incubated with horseradish peroxidase (HRP)-conjugated secondary antibodies for 1 h at room temperature. After washing, the sections were incubated with DAB substrate. Finally, hematoxylin staining was performed after mounting the slides using Permount mounting medium

(Sigma-Aldrich). Cell proliferation was detected also by immunofluorescence staining using an antibody against Ki67 (1:100, ab15580; Abcam) for 2 h. Next, tissue sections were incubated with Alexa Fluor-labeled secondary antibodies (1:500) for 20 min at 37 °C and washed with PBS. The coverslips were mounted in Prolong Gold anti-fade reagent with 4′,6-diamidino-2-phenylindole (DAPI; Invitrogen) for 10 min at room temperature and examined by fluorescence microscopy (Olympus CKX41 and U-RFLT 50).

Western blot analysis

Proteins were extracted from frozen tissue samples by homogenization of the tissues in radioimmunoprecipitation assay (RIPA) lysis buffer. Proteins were also extracted from NPC cells by lysing the cells in RIPA buffer and collecting the supernatant. The protein concentration was estimated using the BCA Protein Assay Kit (Thermo, Waltham, MA, USA). Immunoblotting was performed according to standard procedures. The antibodies used included polyclonal antibodies against β-actin (A5316; Sigma-Aldrich; loading control), LC3 (L7543; Sigma-Aldrich), p62 (Proteintech, Chicago, IL, USA), Bcl-2 (N-19; sc-492; Santa Cruz Biotechnology), Beclin-1 (H-300, sc-11427; Santa Cruz Biotechnology), PI3KC3 (AP8014a; Abgent, San Diego, CA, USA), PI3K-p110 (H-300; sc-134986; Santa Cruz Biotechnology), p-S6 ribosomal protein (Ser235/236; #2211; Cell Signaling Technology, MA, USA), S6 ribosomal protein (5G10, #2217, Cell Signaling Technology), p-mTOR (Ser-2448; sc-101738; Santa Cruz Biotechnology), mTOR (7C10; #2983S; Cell Signaling Technology), p-Akt (Ser-473; sc-7985-R; Santa Cruz Biotechnology), Akt (H-136; sc-8312; Santa Cruz Biotechnology), p38 (A-12; sc-7972; Santa Cruz Biotechnology), p-p38 (D-8; sc-7973; Santa Cruz Biotechnology), and p-GSK3-β (Ser9, #9336, Cell Signaling Technology). The membranes were then incubated with the appropriate HRP-conjugated secondary antibody (diluted 1:20,000) (IRDy; LI-COR) for 45 min. Finally, antigens were visualized on a near-infrared imaging system (Odyssey; LI-COR, Wexford, PA, USA), and data were analyzed using Odyssey 2.1 software (Odyssey; LI-COR).

Statistical analysis

Data are presented as means ± standard deviation. Statistical comparisons between two groups were performed using unpaired Student's *t* tests. Differences among groups were tested by one-way ANOVA analysis of variance with Bonferroni's multiple comparison tests. Moreover, data in cell migration and invasion assays were analyzed by two-way ANOVA analysis of variance with Bonferroni's multiple comparison tests. In all cases, differences were considered statistically significant at $p < 0.05$.

Results

Ang-(1–7) inhibits NPC proliferation in vitro

Cell proliferation was measured by MTT assay (Fig. 1). The anti-proliferative effects of Ang-(1–7) on NPC in vitro were investigated by treating NPC-TW01 cells with a range of doses [0–1.0 μM] of Ang-(1–7) for 24–72 h. Cell viability decreased with increasing concentrations of Ang-(1–7), with a 50% inhibitory concentration of 0.51 μM at 72 h (Fig. 1a). These effects were reversed by coadministration with the MasR antagonist A779 (0.1 and 1.0 μM) at 72 h (Fig. 1b).

Ang-(1–7) inhibits NPC cell migration and invasion in vitro

To determine whether Ang-(1–7) suppresses NPC-TW01 cell migration, a wound healing assay was performed. Scratch wounds were almost the same width in each experimental group at 0 h. Healing and cell migration rate were not significantly reduced in the Ang-(1–7) (0.2 μM) treatment group at 24–72 h (Fig. 2a, b). However, the percentage of wound closure was significantly lower ($p < 0.01$) in the group Ang-(1–7) plus A779 or A779 alone than in the group treated with Ang-(1–7) alone at 48 and 72 h (Fig. 2a, b). To determine whether Ang-(1–7) inhibits NPC-TW01 cells, cell invasion was analyzed by a transwell matrigel invasion assay. Cell invasion in the group treated Ang-(1–7) alone was significantly lower ($p < 0.01$) than in the control group; and lower ($p < 0.01$ or $p < 0.05$) than in the group treated with Ang-(1–7) plus A779 or in the group treated with A779 alone at 24~72 h. Moreover, the ratio with control of transwell cell in Ang-(1–7) alone group was 0.52 (± 0.14), 0.40 (± 0.09), and 0.47(± 0.11) at 24 h, 48 h, and 72 h, respectively, significantly lower than Ang-(1–7) plus A779 group or A779 alone group (Fig. 2c, d). Taken together, these results suggest that Ang-(1–7) inhibits cell migration and invasion in NPC-TW01 cells.

Ang-(1–7) induces Beclin-1/Bcl-2 signaling to activate NPC cell autophagy by upregulating LC3-II expression and downregulating PI3K/Akt/mTOR and p-p38 signaling in vitro

To investigate the signaling pathways involved in autophagy induction in Ang-(1–7)-treated NPC-TW01 cells, Beclin-1 and Bcl-2 protein levels were examined by Western blot. Beclin-1 was upregulated at 24 h and 72 h, whereas Bcl-2 protein levels were lower at 72 h, in 0.2 μM Ang-(1–7)-treated cells relative to the control cells (0 μM) (Fig. 3a, b). We also knocked down Bcl-2 to examine the interaction between Beclin-1 and Bcl-2, which is believed to play a regulatory role in autophagy. siRNA-mediated knockdown of Bcl-2 was

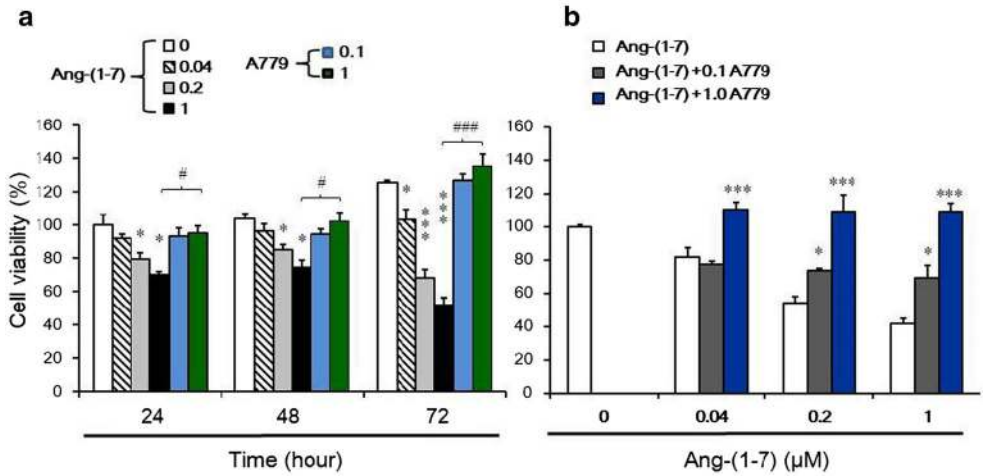

Fig. 1 Effects of Ang-(1–7) on the viability of NPC-TW01 cells in vitro. **a** Cell viability was determined by MTT assay after treatment with various concentrations of Ang-(1–7) for 24, 48, or 72 h. $^{*}p < 0.05$ vs. control; $^{***}p < 0.01$ vs. control; $^{\#}p < 0.05$ vs. 1 μM Ang-(1–7) and $^{\#\#\#}p < 0.01$ vs. 1 μM Ang-(1–7) at 24~72 h. **b** Cell viability was determined after treatment with various concentrations of Ang-(1–7) (0, 0.04, 0.2, and 1 μM) for 72 h and with two concentrations of A779 (0.1 and 1 μM). $^{*}p < 0.05$ and $^{***}p < 0.01$ vs. Ang-(1–7) treated group (0.04, 0.2, and 1 μM)

performed to assess whether Bcl-2 modulates Beclin-1 and LC3-II expression under Ang-(1–7) exposure. Bcl-2 knockdown was confirmed by Western blotting. The levels of Beclin-1 and LC3-II were increased significantly in cells treated with 0.2 μM Ang-(1–7) and Bcl-2 siRNA (Fig. 3e, f). These findings suggest that Ang-(1–7) activates autophagy in NPC-TW01 cells by modulating the Beclin-1/Bcl-2 complex. In addition, Western blot analysis indicated that the ratio of LC3-II to LC3-I was significantly higher following treatment with 0.2 μM Ang-(1–7) compared with the controls at 24 h and 72 h, and LC3-II expression was lower in the Ang-(1–7) plus A779 coadministration and A779 alone groups than in the Ang-(1–7) alone group at 72 h (Fig. 3a, b). In reverse, p62 expression was lower in the 0.2 μM Ang-(1–7)-treated cultures than in the controls at 24 h and 72 h, and the level of p62 in the Ang-(1–7) plus A779 coadministration and A779 alone groups was higher than in the Ang-(1–7) alone group at 72 h (Fig. 3a, b). Taken together, these data suggest that autophagy is activated in NPC-TW01 cells after prolonged Ang-(1–7) treatment. We also investigated whether the effects of Ang-(1–7) on NPC-TW01 cells are mediated by phosphorylation of proteins involved in this pathway. The phosphorylation of PI3K and S6 ribosomal protein was significantly inhibited by Ang-(1–7) treatment at 24 h and 72 h. The ratios of p-AKT/AKT and p-p38/p38 were significantly decreased following Ang-(1–7) treatment at 72 h, and Ang-(1–7) also reduced p-mTOR expression, suggesting that Ang-(1–7) inhibits the PI3K/Akt/mTOR pathway. Additionally, p38 phosphorylation was affected by Ang-(1–7) treatment at 72 h. However, the results showed that A779 have an ineffective action for members of the PI3K/Akt/mTOR pathway (Fig. 3c, d). Therefore, we designed two mouse models (pre- and post-treatment) to investigate whether Ang-(1–7) induces autophagy in vivo.

Ang-(1–7) inhibits tumor growth in vivo, but not via autophagy, post-treatment

Tumor size was decreased only in the 1 μg/kg Ang-(1–7) post-treatment group (667.7 ± 101.7 mm^3) compared with the mock group (1601.6 ± 223.4 mm^3). In contrast, tumor volume was increased in the 1 μg/kg Ang-(1–7) + A779 Ang-(1–7) post-treatment group (2186.1 ± 521.6 mm^3) (Fig. 4a, b). To examine protein markers of autophagy in vivo, Bcl-2 protein expression was examined by Western blotting. Bcl-2 expression was higher in the 1 μg/kg Ang-(1–7) + A779 Ang-(1–7) post-treatment group than in the mock group. However, no significant differences were observed in other autophagy-associated proteins, including class III PI3K, Beclin-1, LC3, and p62 (Fig. 4c, d).

Pre-treatment with Ang-(1–7) induces autophagy in vivo

Ang-(1–7) pre-treatment (0.2 and 1 μg/kg; tumor size 59.2 ± 47.2 and 805.7 ± 107.8 mm^3, respectively) significantly reduced the tumor size compared with the mock group (1458.4 ± 213.9 mm^3), and this effect was reversed by A779 coadministration (1826.1 ± 570.8 mm^3) (Fig. 5a, b). The protein levels of class III PI3K and LC3-II (in the 1 μg/kg Ang-(1–7) pre-treatment group) and Beclin-1 (in the 0.2 or 1 μg/kg Ang-(1–7) pre-treatment group) were increased relative to those in the mock group, whereas the expression of Bcl-2 and p62 was decreased in both

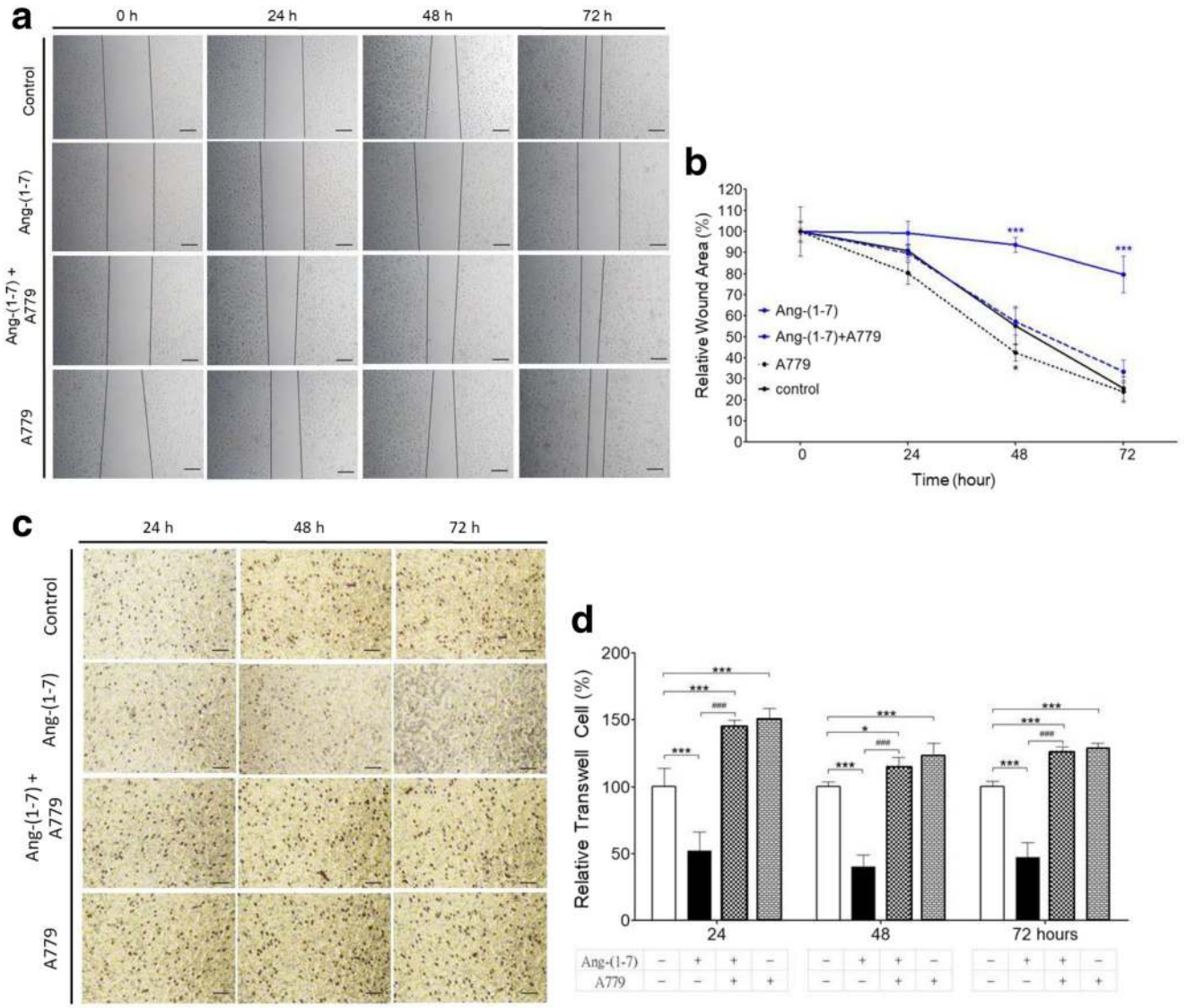

Fig. 2 Effects of Ang-(1–7) on cell migration and invasion of NPC-TW01 cells in vitro. **a** Cell migration was determined using a wound healing assay after treatment of NPC-TW01 cells with control, Ang-(1–7) (0.2 μM) alone, Ang-(1–7) plus A779 (1 μM) or A779 (1 μM) alone for 24, 48, or 72 h. Scale bar = 100 μm. **b** Quantification of the percentage of wound closure in each group. $^{***}p < 0.01$ in Ang-(1–7) alone group vs. other groups at 48 h and 72 h. **c** Transwell matrigel invasion assay of NPC-TW01 cells treated with control, Ang-(1–7) alone, Ang-(1–7) plus A779 (1 μM) or A779 (1 μM) alone. Scale bar = 50 μm. **d** Quantification of cell migration (transwell) in each group. $^{*}p < 0.05$ and $^{***}p < 0.01$ vs. control at 24 ~72 h; $^{\#\#\#}p < 0.01$ vs. Ang-(1–7) at 24 ~72 h

Ang-(1–7) pre-treatment groups (Fig. 5c, d). The effect of all protein levels was reversed in the Ang-(1–7) pre-treatment group following pre-treatment with Ang-(1–7) + A779 (Fig. 5c, d). Moreover, to identify cell proliferation and autophagy, Ki67 and LC3-II expression was assessed by immunofluorescence staining and immunohistochemistry. The intensity of Ki67 expression (green fluorescence) was weaker in the Ang-(1–7) and Ang-(1–7) + 5 μg/kg 3-MA pre-treatment groups than in the mock and Ang-(1–7) + A779 pre-treatment groups according to both immunofluorescence staining (Fig. 5e: left panel) and immunohistochemistry (Fig. 5e: middle panel). LC3-II staining was more intense in the Ang-(1–7) and Ang-(1–7) + 3-MA pre-treatment groups compared with the mock and Ang-(1–7) + A779 pre-treatment groups. Therefore, these results suggest that pre-treatment with Ang-(1–7) may induce autophagy in vivo.

Pre-treatment with Ang-(1–7) downregulates phosphorylation of PI3K/Akt/mTOR pathway effectors in vivo

The PI3K/Akt/mTOR pathway plays an important role in regulating cell death, including apoptosis and autophagy. Therefore,

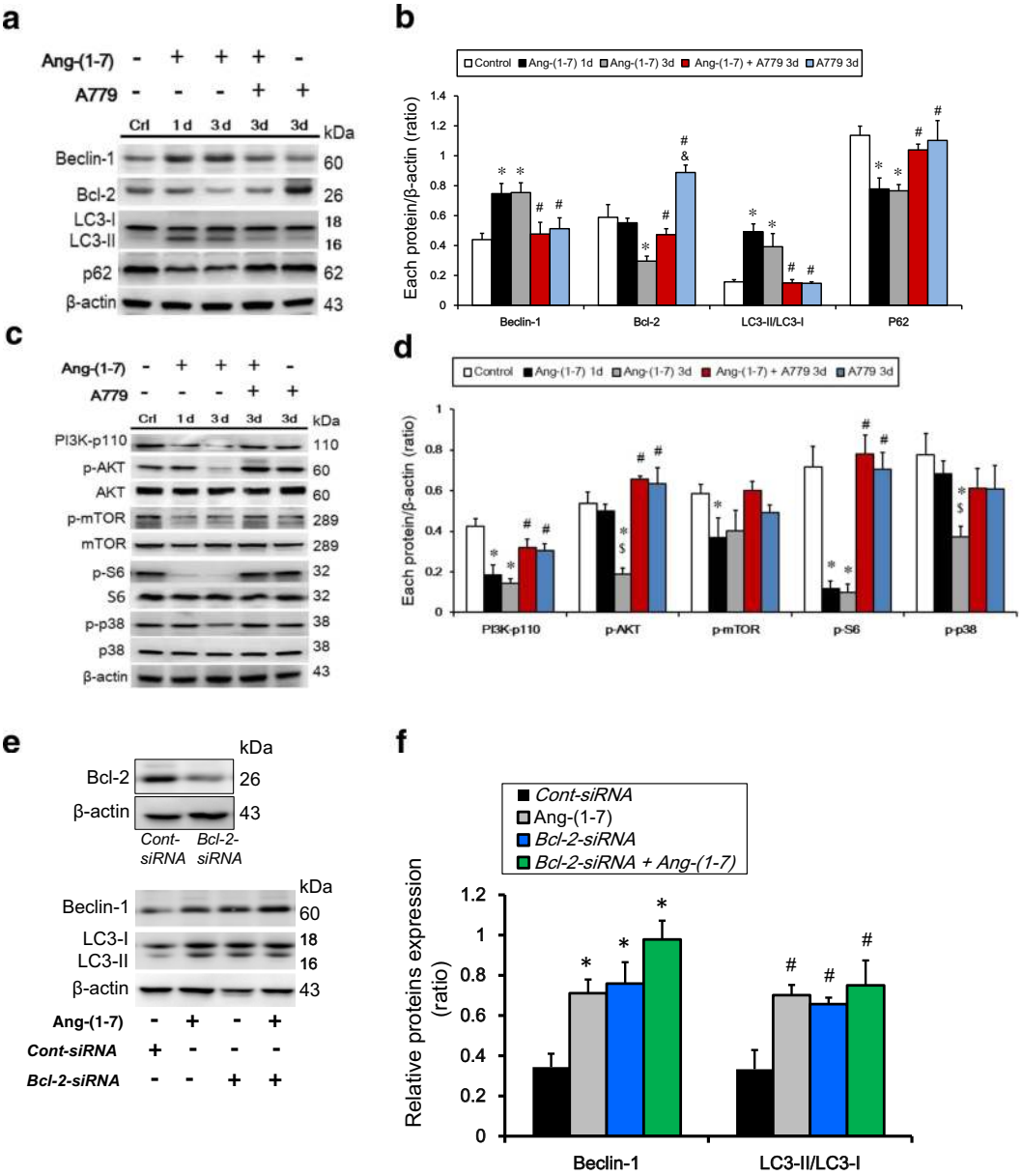

Fig. 3 Effects of Ang-(1–7) on autophagy of NPC-TW01 cells in vitro. Ang-(1–7) may downregulate members of the PI3K/Akt/mTOR pathway and p-p38 in NPC-TW01 cells. **a**, **b** Cells were treated with Ang-(1–7) (0.2 μM) for 24 h (1 d) and 72 h (3 d), Ang-(1–7) plus A779 coadministration and A779 alone for 72 h (3 d), the protein levels of Bcl-2, Beclin-1, LC3, p62, PI3K-p110, p-Akt, Akt, p-S6, S6, p-mTOR, mTOR, p-p38, and p38 were determined by Western blotting. **b**, **d** Quantification of the band intensities for Beclin-1, LC3-II, Bcl-2, p62, PI3K-p110, p-Akt, p-p38, p-S6, and p-mTOR. Results are presented as the mean ± standard deviation (SD) of three experiments. $^{*}p < 0.05$ vs. control; $^{\#}p < 0.05$ vs. Ang-(1–7) at 72 h (3 d); $^{\$}p < 0.05$ vs. Ang-(1–7) at 24 h (1d). **e**–**f**) Knockdown of Bcl-2 in NPC-TW01 cells and resulting expression levels of Beclin-1. Knockdown of Bcl-2 was confirmed by Western blotting. Quantification of the band intensities for Beclin-1 and LC3-II protein expression in NPC-TW01 cells; $^{*}p < 0.05$, $n = 3$. Cont-siRNA: control siRNA

we investigated whether the effects of Ang-(1–7) pre-treatment are mediated by the phosphorylation of protein effectors using a tumor xenograft mouse model. The phosphorylation of Akt, p-GSK3-β and mTOR was inhibited by pre-treatment with Ang-(1–7). This effect was reversed in the Ang-(1–7) + A779 pre-treatment group. Ang-(1–7) pre-treatment also reduced PI3K expression, suggesting that Ang-(1–7) pre-treatment may inhibit the PI3K/Akt/mTOR pathway. However, p38 phosphorylation was not affected (Fig. 6a, b).

Discussion

A wealth of evidence indicates that Ang-(1–7) plays an important role in cancer pathogenesis. Ang-(1–7) has been

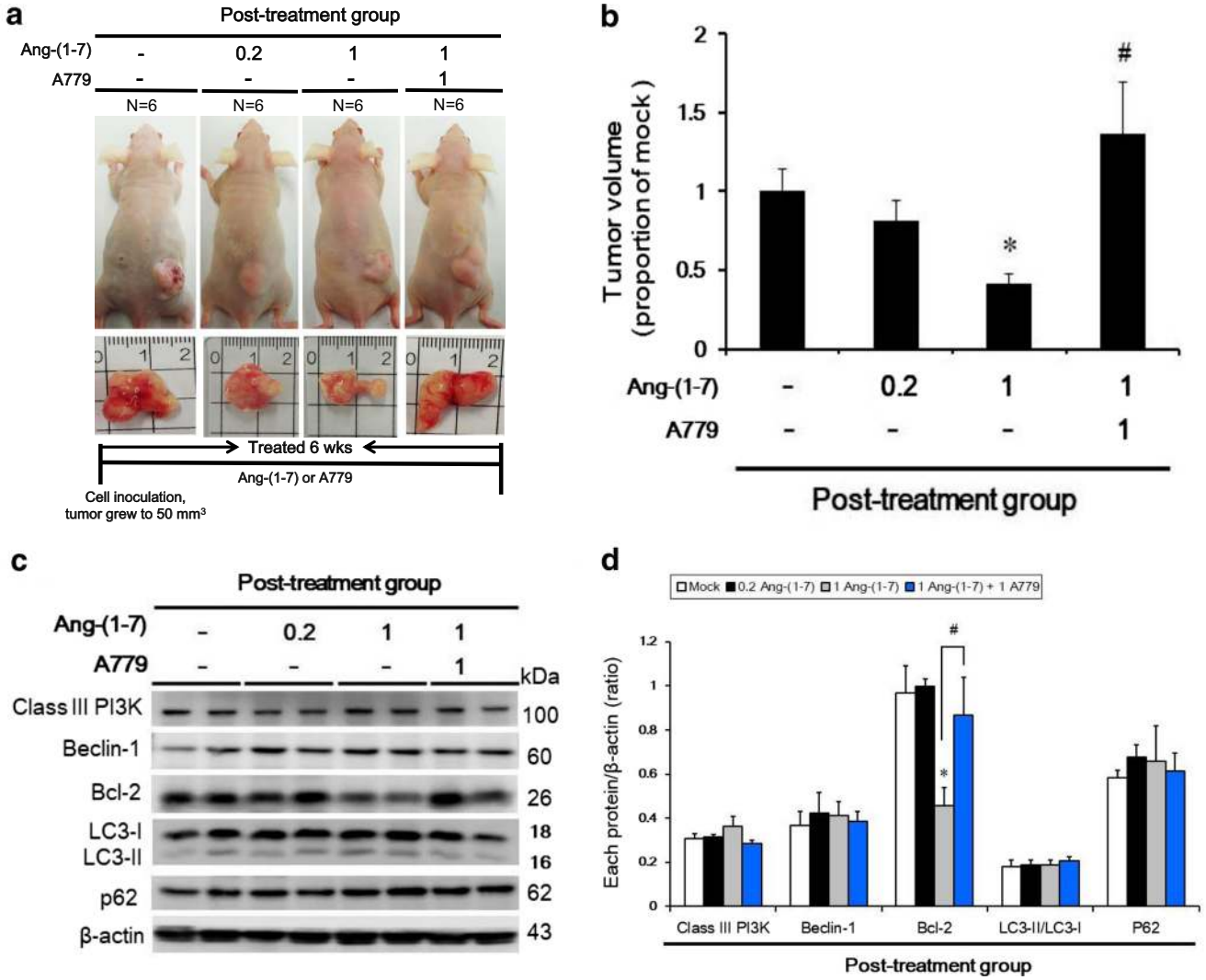

Fig. 4 Ang-(1–7) inhibited tumor size in vivo, but not via autophagy, post-treatment. **a** NPC-TW01 cells were subcutaneously inoculated into the backs of nu/nu mice (post-treatment group; top panel). The bottom panel shows the representative tumor sizes in the four groups. **b** Quantitative analysis of the tumor volume in the post-treatment group. $^{*}p < 0.05$ vs. the mock (saline) group; $^{\#}p < 0.05$ vs. the 1 μg/kg Ang-(1–7) group. **c** Protein expression (class III PI3K, Bcl-2, Beclin-1, LC3-II, and p62) was determined by Western blot analysis. **d** Quantification of the band intensities for class III PI3K, Beclin-1, LC3-II, Bcl-2, and p62. Results are presented as the mean ± SD of three experiments. $^{*}p < 0.05$ vs. the mock group; $^{\#}p < 0.05$ vs. the Ang-(1–7) 1 μg/kg group

identified in a variety of tumors, including lung carcinoma [11–13, 20], prostate cancer [14, 15], breast cancer [21, 22], and hepatocellular carcinoma [16]. Only few studies have demonstrated a regulatory function of the RAS in NPC. Wang et al. indicated that AT1R plays a significant role not only in the cell proliferation and invasion, but also in radiation resistance, of NPC cells [23]. No association was found between angiotensin-converting enzyme 2 polymorphisms and the risk of NPC [24]. However, the effects of the RAS on autophagy-associated pathways in NPC remain questionable. Therefore, we designed several experiments to investigate the effects of the Ang-(1–7)/MasR axis on autophagy in NPC both in vitro and in vivo. First, the expression of the RAS receptor in the NPC-TW01 cell line was analyzed by real-time PCR, which showed that the levels of AT1R and MasR

Fig. 5 Pre-treatment with Ang-(1–7) inhibited tumor growth and induced autophagy in vivo. **a** NPC-TW01 cells were subcutaneously inoculated into the backs of nu/nu mice (pre-treatment group; top panel). The bottom panel shows the representative tumor sizes in the four groups. **b** Quantitative analysis of tumor volume in the pre-treatment group. $^{*}p < 0.05$ vs. the mock group; $^{\#}p < 0.05$ vs. the Ang-(1–7) 1 μg/kg group. **c** Protein levels (class III PI3K, Bcl-2, Beclin-1, LC3-II, and p62) were determined by Western blot analysis. **d** Quantification of the band intensities for class III PI3K, Beclin-1, LC3-II, Bcl-2, and p62. Results are presented as the mean ± SD of three experiments. $^{*}p < 0.05$ vs. the mock group; $^{\#}p < 0.05$ vs. the pre-Ang-(1–7) (1 μg/kg) group. **e** Left panel: cell proliferation in mouse tumor tissues evaluated by Ki67 immunofluorescence (green) and DAPI staining (blue, nuclei). Scale bar = 50 μm. Middle panel: cell proliferation evaluated by Ki67 immunohistochemistry. Scale bar = 60 μm. Right panel: cell autophagy in mouse tumor tissues evaluated by LC3-II immunohistochemistry. Scale bar = 30 μm

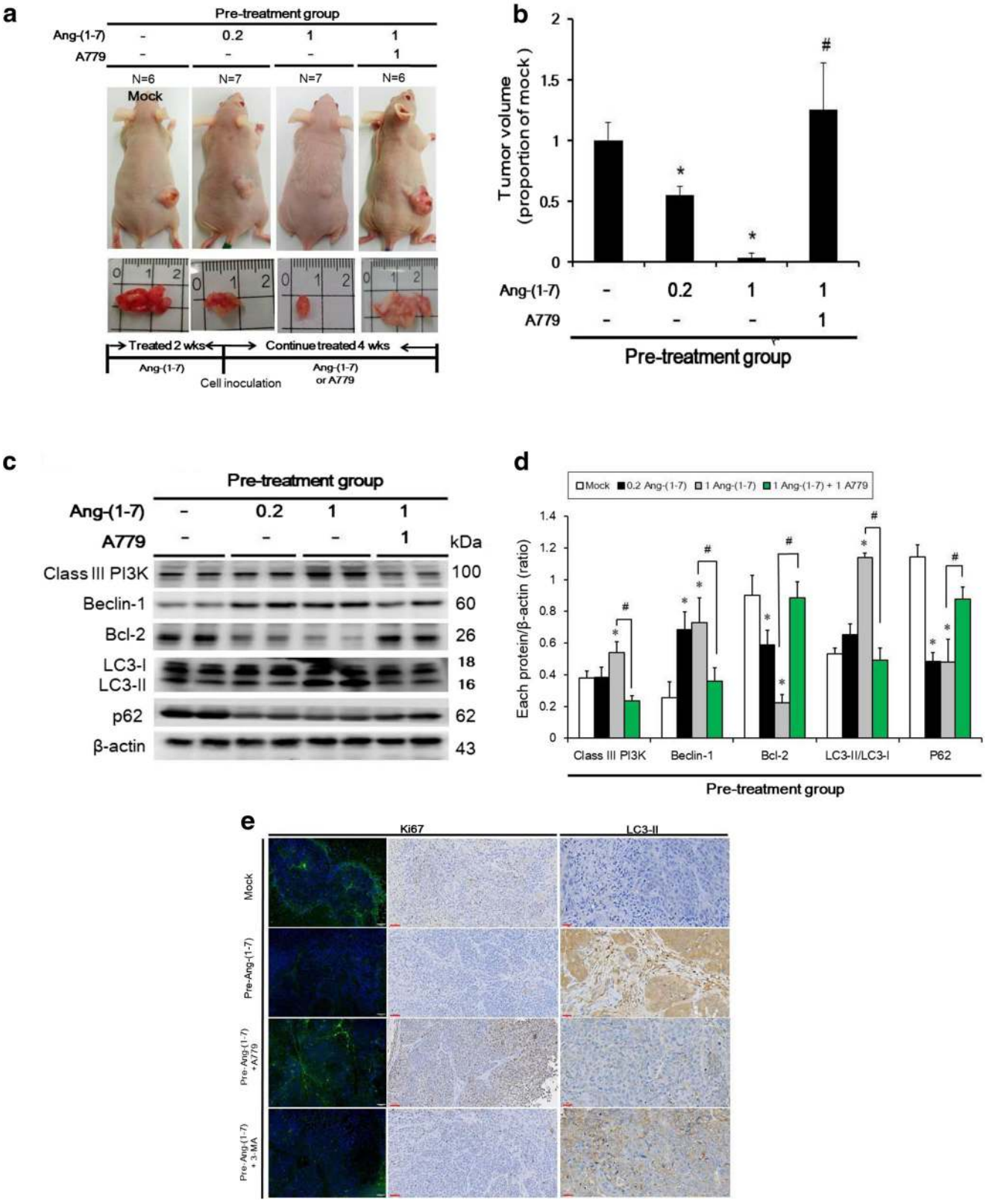

were 2.5-fold higher than that of the AT2 receptor (Fig. S1). We also examined MasR expression in the Ang-(1–7)/MasR axis in the NPC-TW01 cell and human nasopharyngeal xenografts, which revealed that Ang-(1–7) upregulated MasR

expression in vitro and in vivo (Fig. S2). Second, we revealed that Ang-(1–7) at low concentrations (0.04, 0.2 and 1 μM) inhibited cell viability, migration, and invasion in NPC-TW01 cells (Figs. 1 and 2). These results are consistent with a previous study, which reported that Ang-(1–7) upregulated the mRNA level of MasR. Moreover, treatment with 0.5 μM Ang-(1–7) significantly decreased H22 murine hepatocellular carcinoma cell proliferation and cell–endothelial cell communication and induced caspase-3 activity [16]. Ang-(1–7) inhibited the migration and invasion of A549 human lung adenocarcinoma cells following treatment with Ang-(1–7) in a dose-dependent manner [12]. Beclin-1 and LC3-II are important members involved in autophagy of mammalian cells [25]. Therefore, we analyzed the expression of these proteins by Western blot analysis in NPC-TW01 cells. Treatment with 0.2 μM Ang-(1–7) for 24 h was significantly upregulated the levels of Beclin-1 and LC3-II and downregulated that of p62. We also examined the expression of the apoptosis-associated proteins pro-caspase-3, pro-caspase-8, and pro-caspase-9. Our data indicate that 2.5 and 5 μM Ang-(1–7) induced a decrease in pro-caspase-3 and -9 expression, respectively, in NPC-TW01 cells. However, pro-caspase-8 expression was not affected (Fig. S3). In addition, the Bcl-2 inhibitor activates the autophagic pathway through the blocking interaction of Bcl-2/Beclin1 and upregulating Beclin-1 [26]. Therefore, by examining the interaction between Bcl-2 and Beclin-1 identified by Bcl-2 siRNA transfection experiments, we found that 0.2 μM Ang-(1–7) caused autophagosome formation because of the increase in LC3-ll levels and induced autophagy via activation of the Beclin-1/Bcl-2 signaling pathway (Fig. 3e). However, concentrations of Ang-(1–7) greater than 2.5 μM triggered NPC-TW01 cell apoptosis due to decreased pro-caspase-3 and -9 expression, confirming that Ang-(1–7) stimulates NPC cell autophagy at lower concentrations.

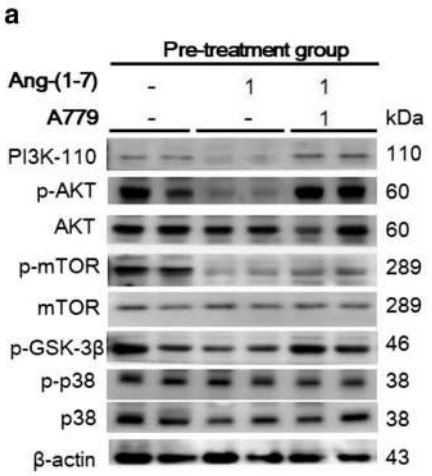

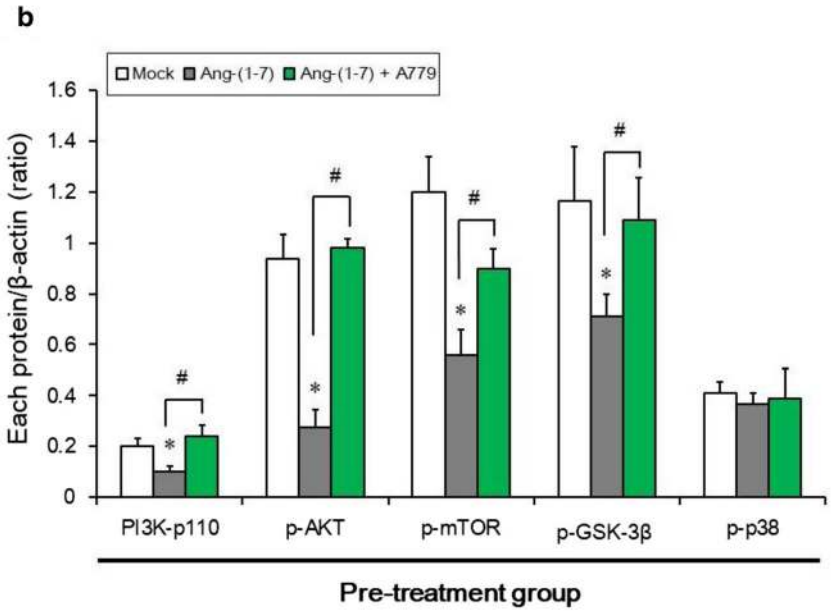

Fig. 6 Pre-treatment with Ang-(1–7) downregulated PI3K/Akt/mTOR pathway members in vivo. **a** Western blot analysis of PI3K, p-Akt, Akt, p-GSK3-β, p-mTOR, mTOR, p-p38, and p38 in the three groups. **b** Quantification of the band intensities for PI3K, p-Akt, p-GSK3-β, p-mTOR, and p-p38. Results are presented as the mean ± SD of three experiments. $^{*}p < 0.05$ vs. the mock group; $^{\#}p < 0.05$ vs. the Ang-(1–7) group

As a downstream effector of Akt, mTOR suppresses autophagy [27, 28]. Ang-(1–7), a peptide with anti-inflammatory properties, plays an important role in the regulation of the tumor microenvironment, and inactivation of the PI3K/Akt and p38 MAPK pathways may be responsible for the inhibitory effects of Ang-(1–7) [12]. In the present study, we investigated whether the effects of Ang-(1–7) in NPC-TW01 cells are mediated by these pathways by examining phosphorylation of the involved proteins. The phosphorylation of PI3K, Akt, p-GSK3-β, and mTOR was inhibited by Ang-(1–7) treatment. Ang-(1–7) also reduced p38 phosphorylation, suggesting that Ang-(1–7) blocks the phosphorylation of proteins involved in the PI3K/Akt/mTOR and p38 pathways (Fig. 3c, d).

The mechanism of Ang-(1–7)-induced cell autophagy remains unclear. In the brain, Ang-(1–7) may help prevent hypertension-induced excessive autophagic activation [29]. In the heart, MasR mediates cardioprotection of Ang-(1–7) against angiotensin II-induced cardiomyocyte autophagy and cardiac remodeling by inhibiting oxidative stress [30]. Ang-(1–7) induced time-dependent upregulation in autophagic activity via LC3-II and Beclin-1 in serum-starved human aortic endothelial cells [31]. Moreover, a recent report indicated that Ang-(1–7) not only causes a significant reduction in the growth of human nasopharyngeal xenografts but also markedly decreases vessel density [19]. Ang-(1–7) may inhibit the growth of human lung adenocarcinoma xenografts in nude mice by reducing cyclooxygenase-2 [13]. In this study, we hypothesized that the regulatory function of the Ang-(1–7)/MasR axis is related to autophagy in NPC in vivo. Therefore, we established two xenograft mouse models (pre- and post-treatment) to evaluate tumor size and autophagy/cell death-associated proteins. A high Ang-(1–7) concentration (1 μg/kg/day) inhibited tumor size post-treatment, but a lower concentration (0.2 μg/kg/day) had no significant effect. However, the expression of autophagy-associated proteins was not affected (Fig. 4). Therefore, we hypothesize that Ang-(1–7) may induce apoptosis by degrading pro-caspase-3 (Fig. S4). In contrast, our results demonstrated that both low- and high-dose Ang-(1–7) inhibited tumor proliferation pre-treatment by directly affecting tumor size and by indirectly inducing autophagy by suppressing the phosphorylation of proteins involved in the PI3K/Akt/mTOR signaling pathway (Figs. 5 and 6). Ang-(1–7) exerted its tumor inhibition effect at a five fold higher concentration post-treatment compared with pre-treatment, suggesting that Ang-(1–7) is more efficient as a preventive than a curative agent in vivo because it caused autophagic activity in NPC.

Ang-(1–7) exerts its anti-proliferative and anti-invasive effects by activating MasR, and A-779, a selective antagonist of MasR, blocks most of these responses to Ang-(1–7) [32]; the concentrations of Ang-(1–7) required to exert its effects are 44.5 and 32.3 pg/ml in women and men, respectively [33], and 15 pg/ml in mice [34]. In addition, Ang-(1–7) is an anti-angiogenic drug with anti-cancer activity that is associated with a reduction in plasma placental growth factor levels at a recommended phase II dose of 400 μg/kg [35]. Ang-(1–7), at a dose of 20 mg daily, was well-tolerated in a phase II trial for the treatment of patients with metastatic sarcoma [36]. In this study, we may use a low-dose of Ang-(1–7) for the pre-treatment model, suggesting alleviation the incidence and reduction in the severity of NPC. Furthermore, while the treatment results for the primary NPC have been encouraging; management of recurrent NPC has been challenging [5, 6]. Therefore, Ang-(1–7) represents a novel preventive agent against NPC via its autophagic effects and may aid in the development of other protective therapeutics against recurrent NPC in the future. Moreover, our results suggest that Ang-(1–7) may provide a preventive treatment in NPC with high risk factors associated with family history, salt-cured fish and meet of diet, smoking or alcohol exposures and infection with the Epstein-Barr virus. However, Ang-(1–7) may exert favorable preventive and antitumor activity of NPC or recurrent NPC in clinical, further clinical investigations are needed in our team.

In conclusion, pre-treatment with a low dose of Ang-(1–7) inhibited tumor proliferation via autophagy induction mediated by the PI3K/Akt/mTOR pathway. Thus, administration of Ang-(1–7) may provide a novel preventive and promising approach for the treatment of NPC or recurrent NPC.

Authors' contributions YTL and CYC: designed the experiments; YTL, HCW and YCH: analyzed the data; YTL: wrote the manuscript; YTL, and HCC performed the experiments; MYY and CYC: review and editing the manuscript. All authors read and approved the final manuscript.

Funding information The authors acknowledge funding received from Kaohsiung Chang Gung Memorial Hospital, Taiwan (grant number: CMRPG8G0791 and CMRPG8G0792), and the Ministry of Science and Technology of Taiwan (grant number: MOST 106-2314-B-182A-063-).

Compliance with ethical standards

Conflict of interest The authors declare that they have no conflict of interest.

References

1. Salehiniya H, Mohammadian M, Mohammadian-Hafshejani A, Mahdavifar N (2018) Nasopharyngeal cancer in the world: epidemiology, incidence, mortality and risk factors. WCRJ 5:e1046
2. Chang MC, Chen JH, Liang JA, Yang KT, Cheng KY, Kao CH (2013) Accuracy of whole-body FDG-PET and FDG-PET/CT in M staging of nasopharyngeal carcinoma: a systematic review and meta-analysis. Eur J Radiol 82:366–373
3. Su WH, Hildesheim A, Chang YS (2013) Human leukocyte antigens and epstein-barr virus-associated nasopharyngeal carcinoma: old associations offer new clues into the role of immunity in infection-associated cancers. Front Oncol 3:299
4. Liao KC, Tsai WL, Fang FM (2017) Quality of life and quality-adjusted life expectancy for patients with nasopharyngeal

carcinoma treated by intensity-modulated radiotherapy - predictive values of clinical stages. IJHNS 1:131–140
5. Yu KH, Leung SF, Tung SY, Zee B, Chua DT, Sze WM, Law SC, Kam MK, Leung TW, Sham JS et al (2005) Survival outcome of patients with nasopharyngeal carcinoma with first local failure: a study by the Hong Kong nasopharyngeal carcinoma study group. Head & Neck 27:397–405
6. Chan JY (2015) Surgical salvage of recurrent nasopharyngeal carcinoma. Curr Oncol Rep 17:433
7. Crowley SD, Coffman TM (2012) Recent advances involving the renin-angiotensin system. Exp Cell Res 318:1049–1056
8. Santos RA, Ferreira AJ, Verano-Braga T, Bader M (2013) Angiotensin-converting enzyme 2, angiotensin-(1–7) and Mas: new players of the renin angiotensin system. J Endocrinol 216:R1–R17
9. Machado RD, Santos RA, Andrade SP (2001) Mechanisms of angiotensin-(1-7)-induced inhibition of angiogenesis. Am J Physiol Regul Integr Comp Physiol 280:R994–R1000
10. Passos-Silva DG, Verano-Braga T, Santos RA (2013) Angiotensin-(1-7): beyond the cardio-renal actions. Clin Sci (Lond) 124:443–456
11. Gallagher PE, Tallant EA (2004) Inhibition of human lung cancer cell growth by angiotensin-(1-7). Carcinogenesis 25:2045–2052
12. Ni L, Feng Y, Wan H, Ma Q, Fan L, Qian Y, Li Q, Xiang Y, Gao B (2012) Angiotensin-(1-7) inhibits the migration and invasion of A549 human lung adenocarcinoma cells through inactivation of the PI3K/Akt and MAPK signaling pathways. Oncol Rep 27:783–790
13. Menon J, Soto-Pantoja DR, Callahan MF, Cline JM, Ferrario CM, Tallant EA (2007) Angiotensin-(1-7) inhibits growth of human lung adenocarcinoma xenografts in nude mice through a reduction in cyclooxygenase-2. Cancer Res 67:2809–2815
14. Krishnan B, Torti FM, Gallagher PE, Tallant EA (2013a) Angiotensin-(1-7) reduces proliferation and angiogenesis of human prostate cancer xenografts with a decrease in angiogenic factors and an increase in sFlt-1. Prostate 73:60–70
15. Krishnan B, Smith TL, Dubey P, Zapadka ME, Torti FM, Willingham MC (2013b) Angiotensin-(1-7) attenuates metastatic prostate cancer and reduces osteoclastogenesis. Prostate 73:71–82
16. Liu Y, Li B, Wang X, Li G, Shang R, Yang J, Wang J, Zhang M, Chen Y, Zhang Y et al (2015) Angiotensin-(1-7) suppresses hepatocellular carcinoma growth and angiogenesis via complex interactions of angiotensin II type 1 receptor, angiotensin II type 2 receptor and mas receptor. Mol Med 21:626–636
17. Hoyer-Hansen M, Jaattela M (2008) Autophagy: an emerging target for cancer therapy. Autophagy 4:574–580
18. Eisenberg-Lerner A, Kimchi A (2009) The paradox of autophagy and its implication in cancer etiology and therapy. Apoptosis 14:376–391
19. Pei N, Wan R, Chen X, Li A, Zhang Y, Li J, Du H, Chen B, Wei W, Qi Y et al (2016) Angiotensin-(1-7) decreases dell growth and angiogenesis of human nasopharyngeal carcinoma xenografts. Mol Cancer Ther 15:37–47
20. Soto-Pantoja DR, Menon J, Gallagher PE, Tallant EA (2009) Angiotensin-(1-7) inhibits tumor angiogenesis in human lung cancer xenografts with a reduction in vascular endothelial growth factor. Mol Cancer Ther 8:1676–1683
21. Cook KL, Metheny-Barlow LJ, Tallant EA, Gallagher PE (2010) Angiotensin-(1-7) reduces fibrosis in orthotopic breast tumors. Cancer Res 70:8319–8328
22. Luo Y, Tanabe E, Kitayoshi M, Nishiguchi Y, Fujiwara R, Matsushima S, Sasaki T, Sasahira T, Chihara Y, Nakae D, Fujii K, Ohmori H, Kuniyasu H (2015) Expression of MAS1 in breast cancer. Cancer Sci 106:1240–1248
23. Wang Q, Zhao W, Wu G (2009) Valsartan inhibits NPC cell line CNE-2 proliferation and invasion and promotes its sensitivity to radiation. Eur J Cancer Prev 18:510–517
24. Li ZH, Pan XM, Han BW, Han HB, Zhang Z, Gao LB (2012) No association between ACE polymorphism and risk of nasopharyngeal carcinoma. J Renin-Angiotensin-Aldosterone Syst 13:210–215
25. Cao Y, Klionsky DJ (2009) Physiological functions of Atg6/Beclin 1: a unique autophagy-related protein. Cell Res 17:839–849
26. Lian J, Wu X, He F, Karnak D, Tang W, Meng Y, Xiang D, Ji M, Lawrence TS, Xu L (2011) A natural BH3 mimetic induces autophagy in apoptosis-resistant prostate cancer via modulating Bcl-2-Beclin1 interaction at endoplasmic reticulum. Cell Death Differ 18:60–71
27. Kim KW, Mutter RW, Cao C, Albert JM, Freeman M, Hallahan DE, Lu B (2006) Autophagy for cancer therapy through inhibition of pro-apoptotic proteins and mammalian target of rapamycin signaling. J Biol Chem 281:36883–36890
28. Yu L, McPhee CK, Zheng L, Mardones GA, Rong Y, Peng J, Mi N, Zhao Y, Liu Z, Wan F et al (2010) Termination of autophagy and reformation of lysosomes regulated by mTOR. Nature 465:942–946
29. Jiang T, Gao L, Zhu XC, Yu JT, Shi JQ, Tan MS, Lu J, Tan L, Zhang YD (2013) Angiotensin-(1-7) inhibits autophagy in the brain of spontaneously hypertensive rats. Pharmacol Res 71:61–68
30. Lin L, Liu X, Xu J, Weng L, Ren J, Ge J, Zou Y (2016) Mas receptor mediates cardioprotection of angiotensin-(1-7) against angiotensin II-induced cardiomyocyte autophagy and cardiac remodelling through inhibition of oxidative stress. J Cell Mol Med 20:48–57
31. Wang HJ, Chen SF, Lo WY (2016) Identification of cofilin-1 induces G0/G1 arrest and autophagy in angiotensin-(1-7)-treated human aortic endothelial cells from iTRAQ quantitative proteomics. Sci Report 6:35372
32. Tallant EA, Ferrario CM, Gallagher PE (2007) Angiotensin-(1-7) inhibits growth of cardiac myocytes through activation of the mas receptor. Am J Physiol Heart Circ Physiol 289:1560–1566
33. Sullivan JC, Rodriguez-Miguelez P, Zimmerman MA, Harris RA (2015) Differences in angiotensin-(1–7) between men and women. Am J Physiol Heart Circ Physiol 308:H1171–H1176
34. Fang C, Stavrou E, Schmaier AA, Grobe N, Morris M, Chen A, Nieman MT, Adams GN, LaRusch G, Zhou Y, Bilodeau ML, Mahdi F, Warnock M, Schmaier AH (2013) Angiotensin 1-7 and Mas decrease thrombosis in Bdkrb2-/- mice by increasing NO and prostacyclin to reduce platelet spreading and glycoprotein VI activation. Blood 121:3023–3032
35. Petty WJ, Miller AA, McCoy TP, Gallagher PE, Tallant EA, Torti FM (2009) Phase I and pharmacokinetic study of angiotensin-(1-7), an endogenous antiangiogenic hormone. Clin Cancer Res 15:7398–7404
36. Savage PD, Lovato J, Brosnihan KB, Miller AA, Petty WJ (2016) Phase II trial of angiotensin-(1-7) for the treatment of patients with metastatic sarcoma. Sarcoma 2016:4592768